p-type Ge cyclotron-resonance laser: Theory and experiment

P. Pfeffer and W. Zawadzki
Institute of Physics, Polish Academy of Sciences, 02-668 Warsaw, Poland

K. Unterrainer,* C. Kremser,* and C. Wurzer
Institut für Experimentalphysik, Universität Innsbruck, A-6020 Innsbruck, Austria

E. Gornik
Walter Schottky Institute, TU-München, D-8046 Garching, Germany

B. Murdin and C. R. Pidgeon
Heriot Watt University, Edinburgh, Scotland
(Received 17 July 1992)

p-type germanium in crossed magnetic and electric fields is used as a continuously tunable laser source in the far infrared. To describe magneto-optical transitions responsible for the laser action, we use the complete version of the Pidgeon and Brown model, which accounts for the nonparabolicity and nonsphericity of the Γ_8 valence bands in Ge. It is demonstrated that both features are of importance in the correct assignment of the transitions. Also, the heating effects in the light-hole Landau levels are estimated theoretically. The calculations are performed for magnetic fields $\mathbf{B}\|[110]$ and $\mathbf{B}\|[111]$. We compare our theoretical results to experimental work in which we are able to achieve laser action in a tuning range from 28 to 76 cm^{-1} by varying the magnetic field between 1.4 and 3.7 T. The laser output consists of a single line having a width of 0.25 cm^{-1} and a maximum power of about 300 mW for a pulsewidth of 1 μsec. Hall measurements are performed on *p*-type Ge samples with the same configuration as that of the laser crystals in order to determine the effective electric fields involved in the laser action. It is shown that the effective fields differ considerably from the applied fields. We conclude that the laser action, for $\mathbf{B}\|[110]$, at low magnetic fields ($B < 2.7$ T) is governed by the 2-3 transition in the *b* set of light holes, while the action at high fields ($B > 2.8$ T) is governed by the light-hole transition 0-1 in the same set. This agrees with estimations of the population inversion determined by other authors.

I. INTRODUCTION

The use of *p*-type germanium in crossed electric and magnetic fields as a source of stimulated tunable emission in the far infrared has recently become a subject of intensive studies.[1] The cyclotron resonance (CR) laser based on light-hole transitions between Landau levels exhibits a narrow-band spectrum which is linearly tunable by the magnetic field; the light–heavy-hole laser is based on transitions between the light- and the heavy-hole bands and shows a broadband emission spectrum.

An important requirement for establishing an inverted population of Landau levels is that the latter have an unequal energy spacing. In the valence band of Ge that is automatically the case, since the degeneracy of the Γ_8 band gives rise to the Luttinger (or "quantum") effects.[2] The Landau-level spacing in this case is influenced also by the electric field.[3] In the theoretical work of Vosilyus and Levinson[4] and Kurosawa and Maeda,[5] an inverted carrier distribution in the case of streaming motion in crossed electric and magnetic fields was predicted. The basic idea was that a scattering free transit of carriers up to the energy of the strong scattering threshold (optical-phonon emission) can provide an inverted hot-carrier distribution.

The first experimental success was the observation of the light-hole–heavy-hole laser by Andronov *et al.*[6] and Komiyama, Iizuka, and Akasaka.[7] The first experimental discovery of stimulated CR emission from light holes in Ge was made by Vasil'ev and Ivanov.[8] By further investigations of this radiation, including the analysis of the spectrum, stimulated emission could be confirmed in the frequency range between 30 and 50 cm^{-1}.[9] Mityagin *et al.*[10] reported stimulated Landau emission from light holes in *p*-Ge in the frequency range between 70 and 90 cm^{-1}. More recently, Unterrainer *et al.*[11] reported on strong stimulated cyclotron resonance emission with an output power of several 100 mW for the magnetic field parallel to the [110] crystallographic direction of the Ge laser crystals. Mel'nichuk *et al.*[12] showed that quantum effects caused by the mixing of the light and heavy holes play an important role in the buildup of a population inversion.

The CR laser emission has usually been observed in two magnetic-field regions, depending on sample doping. We will call them low-field (1.5–2.5 T) and high-field (3.5–4.5 T) regions. This corresponds to respective higher and lower electric fields. In general, lower impurity concentration samples oscillate at lower fields and vice versa.

The theoretical description of electrons in semiconductors in the presence of crossed electric and magnetic fields has by now a fairly long history. The first paper on the subject was by Hensel and Peter[13] who, using second-order perturbation theory, showed that in the degenerate valence bands of Ge a transverse electric field has a nontrivial effect on the Landau levels. In an important paper Aronov[14] observed that, since the shift of Landau levels in an electric field has opposite signs for electrons and holes, it should be observable in interband optical transitions. This was followed by Shindo[15] and Vrehen,[16] who also treated the presence of the electric field by perturbation theory. Vrehen, Zawadzki, and Reine[3] calculating the light-hole Landau energies in Ge went beyond this approach and demonstrated that the electric field tends to remove the Luttinger effects (i.e., the unequal spacings of Landau levels at low quantum numbers n, cf. Luttinger[2]). Zak and Zawadzki[17] examined the one-band effective-mass approximation for electrons in crossed fields, on which the whole previous work had been based (cf. Luttinger and Kohn[18]). They showed that this approximation is valid only for sufficiently low values of the E/B ratio. Zawadzki and Lax[19] treated the case of high E/B values, using a model of two interacting energy bands. This model predicts a destruction of Landau levels by sufficiently strong electric field (cf. also Praddaude,[20] Aronov and Pikus[21]). This effect was demonstrated on InSb by Zawadzki, Mahn, and Merkt.[22] On the other hand, following a prediction of Zawadzki,[23] Merkt[24] showed that in the nonparabolic conduction band of InSb the electric field induces harmonics of the cyclotron resonance.

The theoretical work related to the tunable cyclotron resonance laser in crossed fields is concentrated on the valence bands of Ge. Since the shift of Landau levels in a transverse electric field is proportional to the effective mass, the shifts of light- and heavy-hole levels are very different, resulting in many anticrossing events, the solution to the problem must be obtained numerically. The technique applied was that of Evtuhov,[25] looking for solutions in the form of sums of harmonic-oscillator functions. This way one transforms the initial differential eigenvalue problem into diagonalization of a large number matrix. The above method was used by Stoklitski[26] and by Kuroda and Komiyama.[27] The initial Hamiltonian was that of Luttinger.[2] However, at magnetic fields used to operate the CR laser this approach is not adequate since the nonparabolicity of the light-hole valence band of Ge becomes important. This feature was taken into account by Unterrainer *et al.*,[11] who used the magnetic solutions of the Pidgeon and Brown model[28] and included the electric field by perturbation theory. This approach was developed further by Murdin *et al.*[29]

In this paper we present the theoretical description of the Landau energies in crossed fields based on the complete coupled band model, fully accounting for the nonparabolicity and nonsphericity of the valence bands in Ge. We show also the newest experimental data on the CR laser, in particular the possibility of a continuous tuning between 28 and 90 cm^{-1} and compare them to our theoretical results. The effective electric fields in the lasing regime have been determined by measuring the Hall fields and have been used in the calculations.

The paper is organized in the following way. Section II contains the outline of the theory. Section III presents experimental data, both on the laser emission and on Hall measurements. In Sec. IV we compare the results on laser emission with the calculations and identify the transitions involved. We conclude with a short summary.

II. THEORY

The Hamiltonian for a semiconductor electron in the presence of a periodic lattice potential $V_0(\mathbf{r})$ and external magnetic and electric fields reads as

$$H=\frac{1}{2m_0}(\mathbf{p}+e\,\mathbf{A})^2+V_0(\mathbf{r})+H_{\mathrm{SO}}+\mu_B\mathbf{B}\cdot\boldsymbol{\sigma}+e\mathbf{E}\cdot\mathbf{r}\ , \quad (1)$$

where $\mathbf{A}$ is the vector potential of the magnetic field $\mathbf{B}$, H_{SO} is the spin-orbit (SO) interaction, and $\boldsymbol{\sigma}$ denotes the Pauli spin operator. We work in the Luttinger-Kohn representation, looking for solutions in the form

$$\Psi=\sum_l f_l(\mathbf{r})u_{l0}(\mathbf{r})\ , \quad (2)$$

where f_l are the envelope (slowly varying) functions and u_{l0} are the periodic Luttinger-Kohn amplitudes. In the Luttinger-Kohn basis the electric potential $e\mathbf{E}\cdot\mathbf{r}$ has only diagonal components (cf. Zak and Zawadzki[17]).

Our theoretical approach is based on the Pidgeon and Brown[28] and Weiler, Aggarwal, and Lax[30] coupled-band description. This model of the band structure at the Γ point of the Brillouin zone takes explicitly into account the Γ_6 conduction band, the Γ_8 valence, the Γ_7 split-off valence band, and incorporates far bands in the k^2 approximation. The energy bands resulting from the model are nonparabolic and nonspherical. In addition to the presence of a magnetic field, for which this description has been applied until the present, we include the electric field in the transverse configuration.

As in the case of free electrons, one takes the magnetic field in the $\mathbf{z}$ direction. If the Landau gauge for the vector potential is $\mathbf{A}=(0,-By,0)$, it is convenient to take the electric field $\mathbf{E}$ in the y direction, so that the electric potential is $V=eEy$. One can then separate out the x and z variables by looking for solutions in the form $f(\mathbf{r})=\exp(ik_x x+ik_z z)\varphi(y)$ and solve the remaining one-dimensional equations. Thus, the quantum numbers (apart from the spin) are n,k_x,k_z, just as in the case of the magnetic field alone.

The eigenvalue problem for the electron in crossed fields has the general form

$$\sum_{l=1}^{8}(D_{l'l}+e\mathbf{E}\cdot\mathbf{r}\delta_{l'l})f_l=\varepsilon f_{l'}\ ;l'=1,\ldots,8 \quad (3)$$

where D in our model is an 8×8 differential matrix. For $\mathbf{B}$ parallel to the [110] crystal direction (which is the configuration of our interest) and for $k_x=k_z=0$ (which corresponds to the maximum density of states) the matrix D factorizes into two 4×4 matrices $D(a)$ and $D(b)$.

These describe two sets of levels, the a set and the b set, corresponding to two projections of the effective spin on the magnetic-field direction. It is usually convenient to break the D matrices into sums: $D(a)=D_0(a)+D_1(a)$, and $D(b)=D_0(b)+D_1(b)$. The separation is done in such a way that the eigenvalue problem for $D_0(a)$ [or $D_0(b)$] is satisfied by a column of four harmonic-oscillator functions. The matrices $D_0(a)$ and $D_0(b)$ partially include the anisotropy of the bands. Since the bands at the Γ point are only slightly anisotropic, the matrices $D_1(a)$ and $D_1(b)$, which include the remaining anisotropic terms, are small. Consequently, it has been the general practice to neglect them and consider only the $D_0(a)$ and $D_0(b)$ parts. The eigenvalue problem reduces then to the diagonalization of 4×4 number matrices.

However, we have found from an analysis of magneto-optical data taken on p-Ge that the D_0 matrices do not provide a sufficiently precise description of the Landau levels in the valence bands of Ge at magnetic fields above 3 T. On the other hand, the complete D matrices give a very good description of the data.[31] For this reason, in the present work we also use the complete $D(a)$ and $D(b)$ matrices, as given by Weiler, Aggarwal, and Lax[30] (cf. also Grisar *et al.*[32]).

For **B** parallel to [110] and $k_z=0$ we have Eqs. (4)–(7) as shown below, where $T=\hbar eB/m_0$ and $N=a^+a$. We employ the standard notation, in which a^+ is the raising and a is the lowering operator for the harmonic oscillator functions and μ^+ is the Hermitian conjugate of the operator μ. The following definitions are used:

$$\gamma'=(\gamma_2+3\gamma_3)/4,\quad \gamma''=(3\gamma_2+5\gamma_3)/8\ ,$$
$$q_1=-3Tq,\quad q_2=(3\sqrt{3}/8)Tq,\quad q_5=(\tfrac{5}{4})Tq\ . \tag{8}$$

Furthermore,

$$\mu_1=3/8T(a^2+a^{+2})(\gamma_3-\gamma_2)\ ,$$
$$\mu_2=-\sqrt{3}/4T(N+\tfrac{1}{2}+3/2a^2)(\gamma_3-\gamma_2)\ . \tag{9}$$

The band parameters are given below. In the notation of Eqs. (4)–(7) we have

$$V=(eEL/\sqrt{2})(a^++a)\ , \tag{10}$$

where $L=\sqrt{(\hbar/eB)}$ is the magnetic radius.

The eigenvalue problem (3) is not soluble in terms of single harmonic-oscillator functions. The reason is that the presence of the electric field and the band anisotropy break the cylindrical symmetry of the system. To solve the problem of eigenvalues we have used, similarly to other workers, the method of Evtuhov,[25] looking for solutions in terms of harmonic-oscillator functions (separately for the a set and b set)

$$f_n=\sum_{l=0}^{\infty}c_l^{(n)}|l\rangle\quad n=1,2,3,4\ . \tag{11}$$

The only nonvanishing matrix elements of the electric-field potential are

$$\langle n|eEy|n\rangle=eEk_xL\ , \tag{12}$$
$$\langle n-1|eEy|n\rangle=\langle n|eEy|n-1\rangle=eEl\sqrt{n/2}\ . \tag{13}$$

One puts the functions (11) into the differential equations, described by (4)–(10), and performs operations prescribed by the operators involved. Next, one multiplies the equations on the left by oscillator functions $\langle 0|$, $\langle 1|$, $\langle 2|$, etc., and integrates the scalar products. This results in linear or algebraic equations for the coefficients $c_l^{(n)}$, which contain the unknown eigenenergy ε. Thus, the initial differential eigenvalue problem is transformed in the standard way into a diagonalization of an infinite number matrix. The general form of this matrix is given by the basic 4×4 block [described by $D_0(a)$ or $D_0(b)$ for the set in question], coupled between different n by the electric term (10) and the small D_1 terms. Since the initial expansion (11) is in terms of magnetic solutions, the convergence of the diagonalization process (i.e., the number of n states to be included) depends strongly on the E/B ratio in question. In the numerical practice we have diagonalized truncated matrices with a size up to 684×684. The corresponding problems in perturbation theory have been discussed by Murdin *et al.*[29]

We have used the following values of the band parameters (cf. Hensel and Suzuki,[33] Aggarwal[34]): $\varepsilon_g=0.888$ eV, $\Delta=0.296$ eV, $\gamma_1=3.32$, $\gamma_2=-0.79$, $\gamma_3=0.66$, $\kappa=-1.62$, $E_p=26.8$ eV, $q=0.06$, $F=-1.1$.

In enumerating the levels we have used the usual convention, in which the highest light-hole levels in both sets are labeled -1, while the highest heavy-hole levels are labeled $+1$.

As already mentioned, the dependence of light-hole Landau energies on the electric field involves a large number of anticrossing events. In consequence, one has

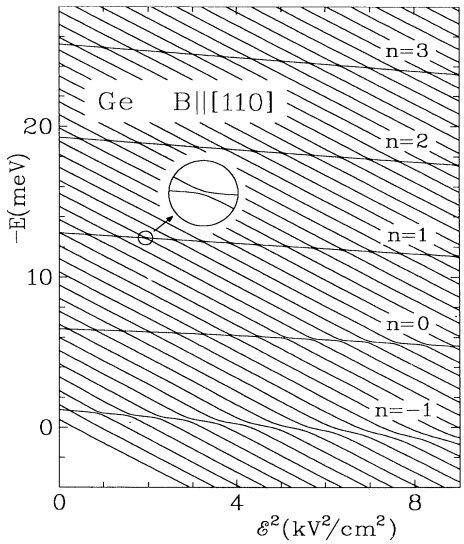

FIG. 1. Light- and heavy-hole Landau level energies (b set) vs the electric field squared at a magnetic filed of 2.5 T, as calculated with the use of the complete Pidgeon and Brown band model.

for set a

$$D_0=\begin{pmatrix} \varepsilon_g+T(N+1)+T2F(n+\frac{1}{2}) & \left[\frac{TE_p}{2}\right]^{1/2}a^+ & -\left[\frac{TE_p}{6}\right]^{1/2}a & \left[\frac{TE_p}{3}\right]^{1/2}a \\ & -T[(\gamma_1+\gamma')(N+\frac{1}{2})+\frac{3}{2}\kappa]+q_1 & T\sqrt{3}\gamma''a^2 & -T\sqrt{6}\gamma''a^2 \\ & & -T[(\gamma_1+\gamma')(N+\frac{1}{2})-\frac{1}{2}\kappa]+q_5 & T\sqrt{2}[\gamma'(N+\frac{1}{2})-\frac{1}{2}\kappa-\frac{1}{2}], \\ & & & -\Delta-T\sqrt{2}[\gamma'(N+\frac{1}{2})-\frac{1}{2}\kappa-\frac{1}{2}] \end{pmatrix} \tag{4}$$

$$D_1=\begin{pmatrix} 0 & 0 & 0 & 0 \\ & \mu_1 & \mu_2^+ +q_2 & -\sqrt{2}\mu_2^+ \\ & & -\mu_1 & -\sqrt{2}\mu_1^+ \\ & & & 0 \end{pmatrix}, \tag{5}$$

and for set b

$$D_0=\begin{pmatrix} \varepsilon_g+TN+T2F(N+\frac{1}{2}) & \left[\frac{TE_p}{6}\right]^{1/2}a^+ & -\left[\frac{TE_p}{2}\right]^{1/2}a & \left[\frac{TE_p}{3}\right]^{1/2}a^+ \\ & -T[(\gamma_1-\gamma')(N+\frac{1}{2})+\frac{1}{2}\kappa]-q_5 & T\sqrt{3}\gamma''a^2 & -T\sqrt{2}[\gamma'(N+\frac{1}{2})+\frac{1}{2}\kappa+\frac{1}{2}] \\ & & -T[(\gamma_1+\gamma')(N+\frac{1}{2})-\frac{3}{2}\kappa]-q_1 & T\sqrt{6}\gamma''a^2, \\ & & & -\Delta-T[\gamma'(N+\frac{1}{2})+\kappa+\frac{1}{2}] \end{pmatrix} \tag{6}$$

$$D_1=\begin{pmatrix} 0 & 0 & 0 & 0 \\ & -\mu_1 & \mu_2^+ -q_2 & \sqrt{2}\mu_1^+ \\ & & \mu_1 & \sqrt{2}\mu_2 \\ & & & 0 \end{pmatrix}. \tag{7}$$

to use a smoothing procedure in order to determine an average behavior of the light-hole levels (cf. Fig. 1). This procedure, although reliable, involves a small uncertainty, in particular for the -1 levels in both sets. The smoothing scheme corresponds to the experimental reality of the streaming regime for the heavy holes, in which the Landau levels are strongly broadened, or even washed out.

III. EXPERIMENT

Samples with two different acceptor concentrations were used for the experiments, $N_A - N_D = 8 \times 10^{12}$ cm^{-3} for sample L (low) and $N_A - N_D = 6 \times 10^{13}$ cm^{-3} for sample H (high). The samples were cut from the crystals to form a parallelepiped. The length of the samples parallel to the [110] crystallographic direction was between 20 and 40 mm. The cross section dimensions were 7 and 5 mm parallel to the $[1\bar{1}0]$ and to the [001] directions, respectively. All faces of the samples were polished and were parallel within 30 seconds of arc. Two mirrors were mounted at the sample endfaces to form an additional external resonator. The mirrors consisted of 50-μm-thick Mylar sheets coated by 100-nm gold; one mirror had a central bore (diameter 1mm) serving as output coupler.

The magnetic field was applied parallel to the [110] direction and the electric field parallel to the $[1\bar{1}0]$ direction. Ohmic contacts were made by evaporating indium (with 5% gold) or aluminum onto the (110) faces and alloying at 400 °C.[30] The electric field was applied to the laser crystal in the form of voltage pulses with amplitudes up to 2 kV and a duration of 1 μs by a high-power low-impedance pulse generator. All the experiments were performed at 4.2 K so that the sample was immersed in liquid Helium at the center of a superconducting solenoid. A broadband Ge:Ga detector with a peak sensitivity at about 90 cm^{-1} was used for the measurements of the integral emission intensity. In addition, a photoconductive quantum well detector was used, which was sensitive between 10 and 100 cm^{-1}. The emission spectra were analyzed by a magnetic-field tunable GaAs detector. The Zeeman-split $1s$-$2p^+$ shallow donor line was used for detection. This line is linearly tunable between 45 and 130 cm^{-1} with magnetic fields between 1 and 6.5 T. Due to the fact that the GaAs contains only one species of shallow donors, the absorption is extremely narrow (0.25 cm^{-1}) and thus the GaAs detector can be used as a high-resolution spectrometer.

A. Stimulated CR emission of sample L

The emission intensity of sample L with an impurity concentration of $N_A - N_D = 8 \times 10^{12}$ cm^{-3} was measured by a quantum-well photoconductive detector which was sensitive between 10 and 100 cm^{-1}. In Fig. 2, the range of the external fields where stimulated emission occurs is shown. For electric fields higher than 1.6 kV/cm and magnetic fields higher than 2.75 T we have observed for the first time in a low concentration sample a second emission range. The stimulated emission of the second range extends up to a magnetic field of 3.7 T.

The observation of this second range was made possible by the use of a very homogeneous magnet. The magnetic field was constant within 0.3% over a length of 4 cm. Therefore the variation $\Delta B/B$ of the magnetic field throughout the sample was smaller than the relative linewidth of the stimulated emission $\Delta\nu/\nu = 0.25$ cm^{-1}. Thus absorption losses by noninverted pairs of levels with a resonance energy similar to that of the inverted levels were eliminated.

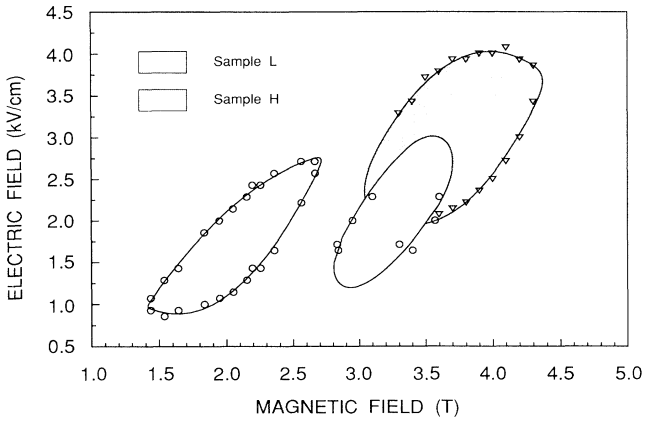

FIG. 2. Ranges of the stimulated far-infrared emission of sample L and sample H as a function of magnetic field for different electric fields. For electric fields higher than 1.6 kV/cm a second emission range at higher magnetic fields is observed for sample L.

In Fig. 3, typical low- and high-field emission spectra are shown for sample L. For both ranges the spectra consist of a single line which tunes with magnetic field. We observe no linewidth difference, but the intensity is 2–3 times higher in the high-field range. In Fig. 4 the emission frequency of sample L is plotted versus the ap-

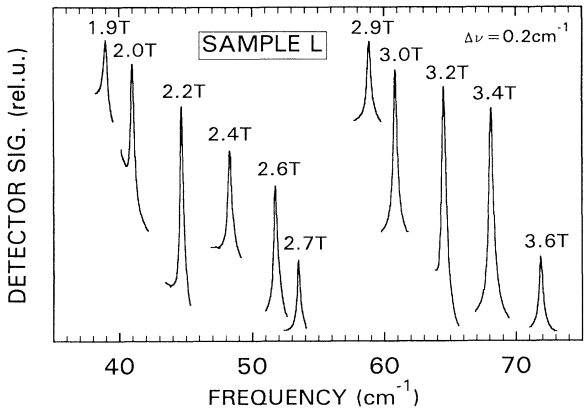

FIG. 3. Spectra of the low- and high-field emission range of sample L, as recorded by the GaAs detector. The spectra consist of magnetically tunable single lines in each range. The applied electric field is varied, 1.7 kV/cm $< E <$ 2.3 kV/cm for magnetic fields, 1.9 T $< B <$ 2.7 T and 1.7 kV/cm $< E <$ 2.5 kV/cm for 2.9 T $< B <$ 3.6 T.

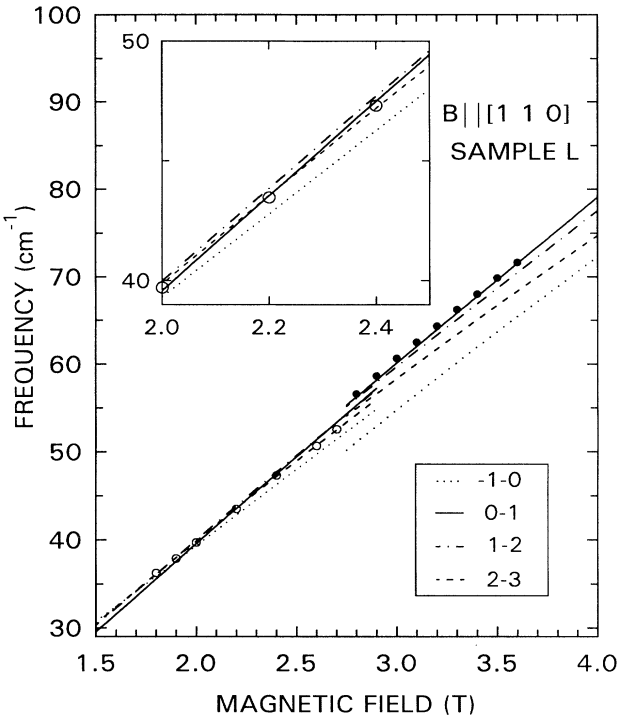

FIG. 4. Emission frequency of sample L as a function of applied magnetic field. Circles indicate the experimental data. The lines show the theoretical results for $n=-1$ to 0, $n=0$ to 1, $n=1$ to 2, and $n=2$ to 3 in the Landau-level transitions in the b set. The electric field is optimized for maximum emission at each experimental point, and the corresponding effective field is evaluated for the computation of transition energies (see Fig. 7).

plied magnetic field. The frequency tunes between 28 and 76 cm^{-1}, which is the largest relative tuning range of stimulated emission reported so far. A tuning range from 30 to 90 cm^{-1} was achieved with the use of an uniaxial stress.[35,36]

It is seen from Fig. 4 that the dependence of the emission frequency on the magnetic field shows a discontinuity between the two ranges at 2.75 T. The corresponding effective cyclotron mass m^l (according to the expression for the CR frequency of the light holes $\hbar\omega_c = eB/m^l$) for the low range at 2.7 T is $m^l = 0.0472m_0$, that of the high range at 2.8 T is $m^l = 0.0461m_0$. It is clear that different pairs of Landau levels are involved in the low-field range ($B < 2.7$ T) and in the high-field range ($B > 2.8$ T) laser transitions. Furthermore, both tunning curves do not go through the origin if extended to the zero magnetic field.

B. Stimulated CR emission of sample H

In sample H with a high impurity concentration of $N_A - N_D = 6\times10^{13}$ cm^{-3}, stimulated cyclotron resonance emission was found for magnetic fields between 3 and 4.5 T (see Fig. 2). As external resonator two Mylar foils coated with gold were used. The power of the stimulated CR emission for this configuration reached 150 mW. Using an external resonator consisting of a spherical mirror and a mesh output coupler we even found an output power of 300 mW for sample H. In general, the power of the emission of the sample H is one to two orders of magnitude larger than that of sample L.

For a detailed analysis of the stimulated CR emission spectra we again used a GaAs detector. There is no linewidth difference to the spectra of sample L. The position of the line is changed in a range between 60 and 90 cm^{-1} by varying the magnetic field. In Fig. 5 the frequency of the emission line is plotted versus the applied magnetic field. The data points are all on one straight line, as expected for CR emission. This line, however, does not go through the origin if extended to zero magnetic field; this represents a change of the effective cyclotron mass m^l of the light holes between $0.0467m_0$ (3 T) and $0.0469m_0$ (4 T). This increase of the effective mass is due to the nonparabolicity effect.

C. Hall field measurements

For an exact theoretical description of the laser action the knowledge of the value of the effective field inside the sample is very important. In order to estimate the effective internal electric field we performed the Hall measurements using samples with the same concentration and the same crystallographic orientation as for the laser crystals. The length of these samples measured only 1 mm. Two additional contacts were attached perpendicular to the contacts for the applied field for the Hall field measurements [Figs. 6(a) and 6(b)]. From these experiments we could determine the value of the resulting field inside the laser crystal (sum of applied field and Hall field) and the direction of the effective field in the (110) plane. Furthermore, we could prove with these results that stimulated emission is directly connected with streaming motion of heavy holes, i.e., stimulated emission stops when streaming motion of the heavy holes disappears. On the other hand, these results are consistent

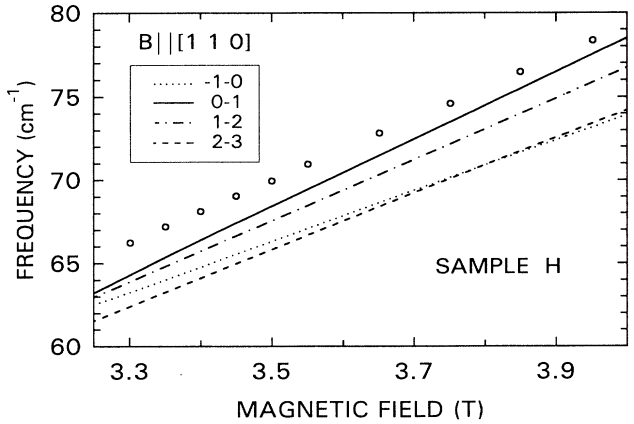

FIG. 5. Emission frequency of sample H vs magnetic field (high-field range) for constant applied electric field ($E_{appl} = 2.643$ kV/cm). The theoretical curves have been calculated using E_{eff} values determined from Fig. 6(b).

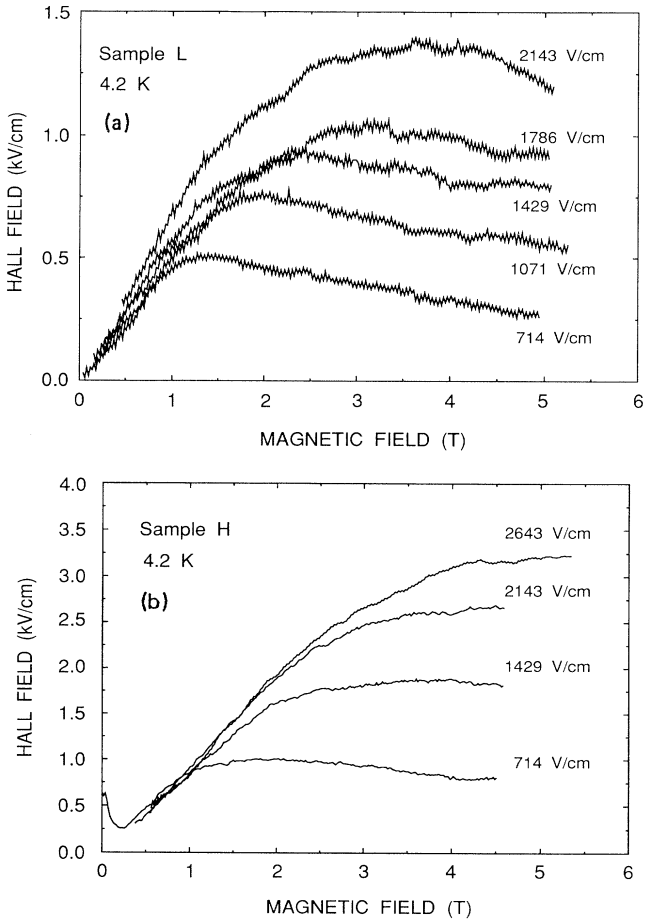

FIG. 6. Hall field vs the applied magnetic field, as measured for different fixed applied electric fields: (a) in sample L ($N_A - N_D = 8\times10^{12}$ cm^{-3}), (b) in sample H ($N_A - N_D = 6\times10^{13}$ cm^{-3}).

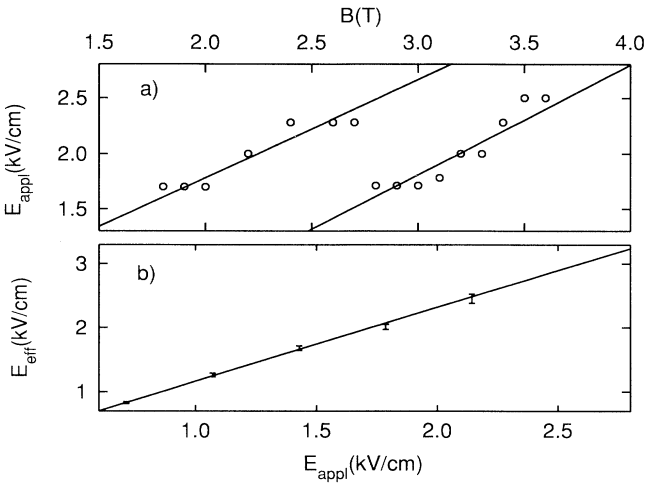

FIG. 7. Dependence of the effective electric field ($E_{\rm eff}$) on the applied magnetic field (B); as used in the calculation for sample L (see Fig. 4). (a) Applied electric field vs magnetic field; circles indicate the experimental points. The solid lines average the experimental points for low and high magnetic fields. (b) Effective electric field ($E_{\rm eff}$) vs applied electric field ($E_{\rm appl}$). The solid lines average the experimental data.

with the critical dependence of the laser action on the crystalographic orientation of the electric field, since the effective mass of the heavy holes determines the rate at which light-hole Landau levels are populated.

IV. RESULTS AND DISCUSSION

A. Results for B|| [110] orientation

We consider first the results for sample L, whose laser frequency was tuned from 28 to 76 cm^{-1}, i.e., in both low and high regions of applied magnetic field. As follows from Fig. 7, the electric field for which the laser action has been observed shows a discontinuity at a magnetic field of about 2.75 T. The discontinuity suggests that the magneto-optical transitions involved in the two regions are not the same. This suggestion is confirmed by the detailed analysis.

In Fig. 4 the experimental laser frequencies are plotted versus magnetic field. The corresponding applied electric field values are read from Fig. 7(a), and the effective values from Fig. 7(b). In Fig. 4 we also show theoretical energies for various light-hole transitions in the b set, as calculated for appropriate B and $E_{\rm eff}$. The best fit to the data in the low-field region is given by the 2 to 3 transition, whereas in the high-field region the data are best described by the 0 to 1 transition. It should be mentioned that it is the D_1 contribution which allows us to discriminate between the 0 to 1 and the 1 to 2 transitions in the high-field range, since without the D_1 terms both transitions have almost the same energy (cf. Refs. 29 and 37). Our calculation spectacularly confirms the results of Mel'nichuk *et al.*,[12] who showed with the use of scattering theory, that for magnetic fields higher than 2.9 T, population inversion is expected between the $n=1$ and the $n=0$ Landau levels. The same transition was recently found in absorption measurements.[31] The transitions we found are also in agreement, in both ranges, with Stoklitskiy's[26] results. He determined the Landau levels with an inverted population by calculating a model distribution function. In the low-field region the theoretical energies for various transitions are close to each other, but the assignment of the 2 to 3 transition is confirmed by an independent set of data (cf. Fig. 8).

It has been generally believed that the Landau levels in the a set do not describe the observed frequencies. We have calculated the transition energies in the a set for the magnetic field of 2.75 T and electric fields on both sides of the discontinuity shown in Fig. 3 [cf. also Fig. 7(a)]. All the transition energies (except one) are in the energy range 51.3–37.9 cm^{-1}, and thus are too low to account for the observed energies. For the 2 to 3 transition and $E_{\rm eff}^2 = 3.25$ (kV/cm)^2 the calculated energy is 53.0 cm^{-1}, which is 2 cm^{-1} below the extrapolated experimental value (from the high-field region). Thus, our calculations confirm that the observed transitions are due to the Landau levels in the b set.

Similar computations to those shown in Fig. 4, but per-

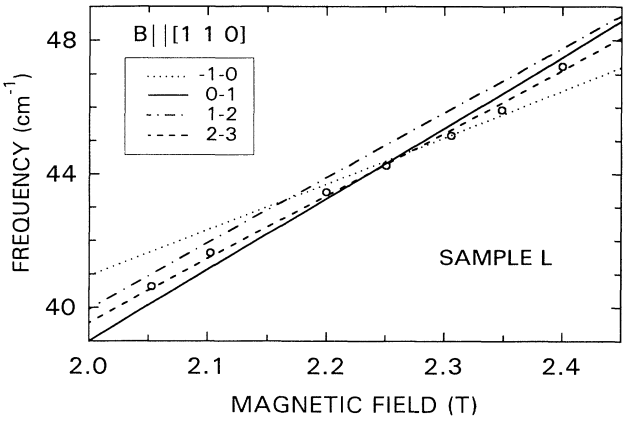

FIG. 8. Emission frequency of sample L vs the applied magnetic field (low-field range) for constant applied electric field ($E_{\text{appl}}=2.143$ kV/cm). The theoretical curves have been calculated using E_{eff}, as determined from Fig. 6(a).

formed with the Luttinger scheme (i.e., neglecting the nonparabolic effects related to the proximity of the conduction and the split-off bands) are shown in Fig. 9. It can be seen that the fit to the data is considerably worse. This confirms that the use of a coupled band scheme is essential for the fields employed in the CR laser.

Figure 8 shows the results for the sample L in the low-field region, obtained at a constant electric field. The effective electric fields used in the calculations have been determined using Fig. 6(a). Similarly to the results shown in Fig. 4, the best fit to the data in this field region is obtained for the 2 to 3 transition.

In Fig. 5 we show the experimental data and calculations for sample H. The electric fields for which stimulated emission occurs are considerably higher than for sample L. The data in the high magnetic-field range are again best described by the 0 to 1 transition, but the calculated energies are 1 to 2 cm^{-1} lower than the experimental ones. The reason for this discrepancy is not quite clear in view of the good agreement for sample L. One possible explanation would be of experimental nature, namely that the E_{eff}, as determined in Fig. 6(b) and used in the calculations, is higher than the real one in the sample. The second, more likely explanation takes into account the fact that at high electric fields one populates higher k_z states of the Landau subbands. These have been neglected until now in our considerations.

Figure 10 shows calculated k_z dependencies of the Landau levels in question (the D_1 terms have been omitted here). It can be seen that the k_z curvatures of various levels are not parallel (apart from the anticrossing events), so that transitions taking place at higher k_z values may have an energy different from that at $k_z=0$. According to a calculation based on the method of Helm, Unterrainer, and Gornik[38] the light holes of Ge in crossed fields of $B=3.6$ T and $E=4$ kV/cm (the average values for the discussed sample H) are heated up to energies of about 15–20 meV above the lowest -1 level (in the inverted energy scale) (see Fig. 11). The 0 to 1 transition energy for k_z values for which E_z ($E_z=\hbar^2k_z^2/2m_0$) is in the range between 0.09 and 0.15 meV (which corresponds roughly to 18.5–20 meV above the -1 level in Fig. 10) is about 1–2 cm^{-1} higher than the transition energy at $k_z=0$. This is what one needs to bring the theory into agreement with the experimental value in Fig. 5. (It should be mentioned that a strictly nonparabolic effect

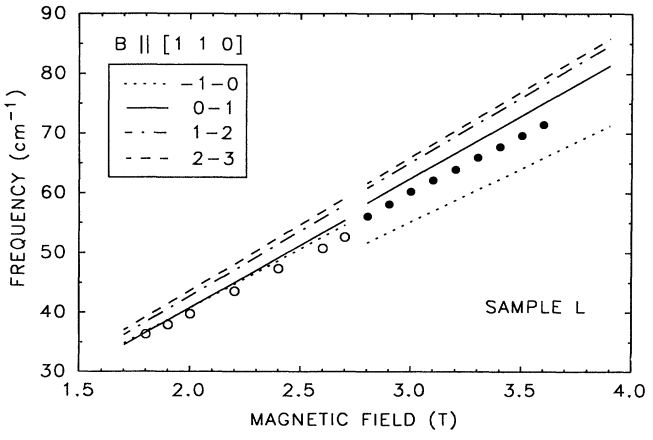

FIG. 9. Emission frequency of sample L vs applied magnetic field. Circles indicate the experimental data. The lines show the theoretical results for the $n=-1$ to 0, $n=0$ to 1, $n=1$ to 2, and $n=2$ to 3 Landau-level transitions (b set), as calculated with the use of the Luttinger band model.

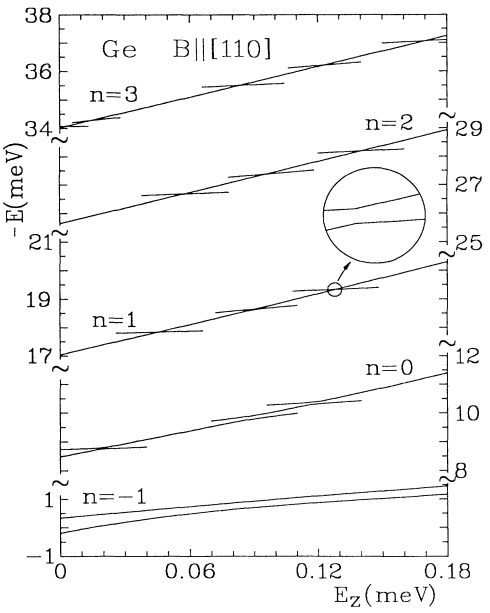

FIG. 10. The k_z dependence of the light-hole Landau levels (b set) calculated on the complete coupled-band model, fully accounting for the nonparabolicity and nonsphericity of the valence bands in Ge for $B=3.6$ T, and $E=4$ kV/cm. ($E_z=\hbar^2k_z^2/2m_0$, where m_0 is the free-electron mass). The 0 to -1 transition energy increases with increasing k_z.

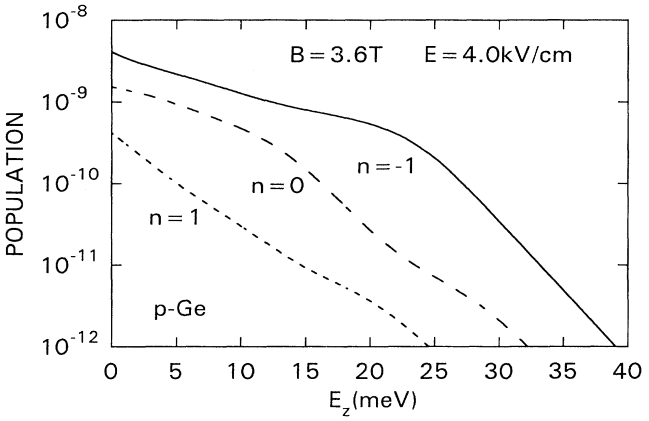

FIG. 11. The calculated one-dimensional distribution function $f_n(k_z)$ for light-hole Landau levels vs $E_z=\hbar^2k_z^2/2m^l(m^l=0.043m_0)$. The calculation does not include the influence of the heavy holes.

would make the transition energy at higher k_z lower than that at $k_z=0$.) The above explanation, although plausible, requires a detailed insight into the complicated processes of the hole heating in p-type Ge in crossed fields.

B. Results for B||[111] orientation

In Fig. 12 we show experimental results of Kuroda and Komiyama,[27] obtained on a Ge sample with $N_A-N_D=4.5\times10^{13}$ cm^{-3} for the field direction **B** parallel to [111]. The figure shows also theoretical transition energies for this case, which we calculated for set b similarly to the **B**||[110] case. The Landau levels were determined using D_0 matrices (cf. Eqs. (4) and (6) with

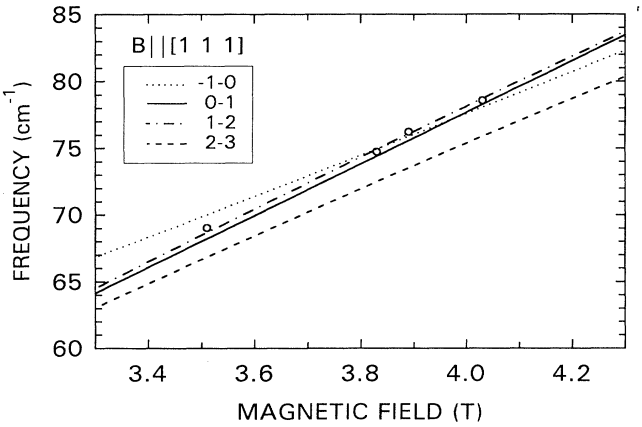

FIG. 12. Emission frequency of a p-Ge Laser ($N_A-N_D=4.5\times10^{13}$ cm^{-3}) vs applied magnetic field for **B**||[111]. Experimental data are those of Kuroda and Komiyama (Ref. 27). The theoretical curves have been calculated for $E_{\rm eff}=4.3$ kV/cm (estimated from average experimental values for $E_{\rm appl}=3$ kV/cm and Figs. 6(a) and 6(b).

$$\gamma'=\gamma_3,\quad \gamma''=(\gamma_2+2\gamma_3)/3\ ,\qquad q_1=-23Tq/8,\quad q_5=13Tq/8\ , \tag{14}$$

and D_1 matrix[30]

$$D_1=\begin{bmatrix}0 & 0 & 0 & 0\\ 0 & \mu_3^+ & q_4 & -\mu_3^+/\sqrt{2}\\ 0 & 0 & -\mu_3^+ & \sqrt{\frac{3}{2}}\mu_3\\ 0 & \sqrt{\frac{3}{2}}\mu_3 & -\mu_3^+/\sqrt{2} & 0\end{bmatrix}, \tag{15}$$

where

$$\mu_3=\sqrt{3}Ta^2(\gamma_3-\gamma_2),\quad q_4=Tq/\sqrt{2}\ .$$

The D_1 terms couple now the $D_0(a)$ and the $D_0(b)$ matrices, which makes the calculation more complicated. We have diagonalized 1368×1368 matrices. The calculations were performed for $E_{\rm eff}=4.3$ kV/cm, which was estimated from the average experimental value of $E_{\rm appl}=3$ kV/cm and Figs. 6(a) and 6(b) (correcting for the different hole concentrations between our samples and the above sample).

The best fit is obtained for the 1 to 2 transition, but the transition 0 to 1 provides an almost equally good description. It should be noted that Kuroda and Komiyama, using the parabolic (Luttinger) band model, identified their data as being due to the −1 to 0 transition (0 to 1 transition in the notation of Ref. 27).

V. SUMMARY

Stimulated emission has been observed between 28 and 76 cm^{-1} in a low concentration sample and between 60 and 90 cm^{-1} at a maximum output power of 300 mW for a high-doped sample. To find theoretical transition energies for the Landau levels in this case we have used for the first time the complete Pidgeon and Brown model as a base of our calculations. We have shown that using only the Luttinger band model gives distinctly different (worse) results. We also found that the inclusion of the D_1 terms to the calculations give nonnegligible corrections to the Landau energies and allows us to discriminate between the transitions responsible for the laser action. A further improvement was made in the theoretical description by using the effective electric-field values, which were determined by the Hall measurements.

On the whole, the coupled-band scheme gives a very good description of the CR laser data both for **B**||[110] and **B**||[111]. We have found that for **B**||[110] the laser action for low magnetic fields ($B<2.7$ T) is governed by the 2 to 3 transition of the light holes in the b set. For high magnetic fields ($B>2.8$ T) the lasing action is attributed to the 0 to 1 transition for the low- and high-doped samples. Furthermore we have shown that for the high-doped samples taking into account the k_z effects can be essential for a quantitative description. This is a possible indication that the inversion does not take place at the

Landau-level band edge ($k_z=0$) for the high concentration samples with high applied electric field. For $\mathbf{B}\|[111]$ and magnetic fields between 3.4 and 4.2 T we assign the laser action to the 1 to 2 transition.

ACKNOWLEDGMENT

One of the authors (P.P.) acknowledges financial support by the Deutscher Akademischer Austauschdienst.

*Present address: Institut für Festkörperelektronik, Technical University Vienna, Austria.

[1] *Infrared Semiconductor Lasers,* edited by E. Gornik and A. A. Andronov [Opt. Quantum Electron. **23**, (1991)].

[2] J. M. Luttinger, Phys. Rev. **102**, 1030 (1956).

[3] Q. M. F. Vrehen, W. Zawadzki, and M. Reine, Phys. Rev. **158**, 702 (1967).

[4] I. I. Vosilyus and I. B. Levinson, Zh. Eksp. Teor. Fiz. **52**, 1013 (1967) [Sov. Phys. JETP **25**, 672 (1967)].

[5] T. Kurosawa and H. Maeda, J. Phys. Soc. Jpn. **31**, 668 (1971).

[6] A. A. Andronov, I. V. Zverev, V. A. Kozlov, Yu. N. Nozdrin, S. A. Pavlov, and V. N. Shastin, Pis'ma Zh. Eksp. Teor. Fiz. **40**, 69 (1984) [JETP Lett. **40**, 804 (1984)].

[7] S. Komiyama, N. Iizuka, and Y. Akasaka, Appl. Phys. Lett. **47**, 958 (1985).

[8] Yu. B. Vasil'ev, and Yu. L. Ivanov, Pis'ma Zh. Tekh. Fiz. **10**, 949 (1984)[Sov. Tech. Phys. Lett. **10**, 398 (1984)].

[9] Yu. B. Vasil'ev, and Yu. L. Ivanov, *Proceedings of the 18th International Conference on the Physics of Semiconductors* (World Scientific, Singapore, 1987), p. 1659.

[10] Yu. A. Mityagin, V. N. Murzin, S. A. Stoklitskiy, and I. E. Trofimov, Pis'ma Zh. Eksp. Teor. Fiz. **46**, 116 (1987) [JETP Lett. **46**, 144 (1987)]; Yu. A. Mityagin, V. N. Murzin, S. A. Stoklitskiy, I. E. Trofimov, and A. P. Chebotarev, in *Proceedings of the 19th International Conference on the Physics of Semiconductors, Warsaw, 1988,* edited by W. Zawadzki (Institute of Physics, Polish Academy of Sciences, Warsaw, 1988), p. 1439.

[11] K. Unterrainer, C. Kremser, E. Gornik, C. R. Pidgeon, Yu. L. Ivanov, and E. E. Haller, Phys. Rev. Lett. **64**, 2277 (1990).

[12] I. M. Mel'nichuk, Yu. A. Mityagin, V. N. Murzin, and S. A. Stoklitskiy, Pis'ma Zh. Eksp. Teor. Fiz. **49**, 486 (1989) [JETP Lett. **49**, 556 (1989);.

[13] J. C. Hensel and M. Peter, Phys. Rev. **114**, 411 (1959).

[14] A. G. Aronov, Fiz. Tverd. Tela (Leningrad) **5**, 552 (1963) [Sov. Phys. Solid State **5**, 402 (1963)].

[15] T. Shindo, J. Phys. Chem. Solids **26**, 1431 (1965).

[16] Q. M. F. Vrehen, Phys. Rev. **145**, 675 (1966).

[17] J. Zak and W. Zawadzki, Phys. Rev. **145**, 536 (1966).

[18] J. M. Luttinger and W. Kohn, Phys. Rev. **97**, 869 (1955).

[19] W. Zawadzki and B. Lax, Phys. Rev. Lett. **16**, 1001 (1966).

[20] H. C. Praddaude, Phys. Rev. **140**, A1292 (1965).

[21] A. G. Aronov and G. E. Pikus, Zh. Eksp. Teor. Fiz. **51**, 281 (1966) [Sov. Phys. JETP **24**, 188 (1967)]; **51**, 505 (1966) [**24**, 339 (1967)].

[22] W. Zawadzki, S. Mahn, and U. Merkt, Phys. Rev. Lett. **55**, 983 (1985).

[23] W. Zawadzki, in *Proceedings of the Ninth International Conference on Physics of Semiconductors, Nauka (Leningrad) 1969* (U.S.S.R. Academy of Sciences, Leningrad, 1969), p. 312.

[24] U. Merkt, Festkörper Probleme Adv. Solid State Phys. **27**, 109 (1986).

[25] V. Evtuhov, Phys. Rev. **125**, 1869 (1962).

[26] S. A. Stoklitskiy, Semicond. Sci. Technol. **7**, B610 (1992).

[27] S. Kuroda and S. Komiyama, Int. J. Infrared Millimeter Waves, **12**, 783 (1991); Semiconductor Sci. Technol. **7**, B618 (1992).

[28] C. R. Pidgeon and R. N. Brown, Phys. Rev. **146**, 575 (1966).

[29] B. N. Murdin, C. R. Pidgeon, K. Unterrainer, C. Kremser, E. Gornik, P. Pfeffer, and W. Zawadzki, J. Modern Opt. **39**, 661 (1992).

[30] M. H. Weiler, R. L. Aggarwal, and B. Lax, Phys. Rev. B **17**, 3269 (1978).

[31] C. Kremser, K. Unterrainer, E. Gornik, P. Pfeffer, W. Zawadzki, B. Murdin, and C. R. Pidgeon, Semiconductor Sci. Technol. (to be published).

[32] R. Grisar, H. Wachering, G. Bauer, J. Wlasak, J. Kowalski, and W. Zawadzki, Phys. Rev. B **18**, 4355 (1987).

[33] J. C. Hensel and K. Suzuki, Phys. Rev. B **9**, 4219 (1974).

[34] R. L. Aggarwal, Phys. Rev. B **2**, 445 (1970).

[35] C. Kremser, K. Unterrainer, E. Gornik, Yu. L. Ivanov, C. R. Pidgeon, C. Meny, and J. Leotin, in *Proceedings of the 20th International Conference on the Physics of Semiconductors,* edited by E. M. Anastassakis and J. D. Joannopoulos (World Scientific, Singapore, 1990), p. 2467.

[36] V. I. Gavrilenko, Z. F. Krasilnik, and V. V. Nikonorov, in *Proceedings of the 20th International Conference on the Physics of Semiconductors* (Ref. 35), p. 2483.

[37] K. Unterrainer, C. Kremser, C. Wurzer, E. Gornik, P. Pfeffer, W. Zawadzki, B. Murdin, and C. R. Pidgeon, Semicond. Sci. Technol. **7**, B604 (1992).

[38] M. Helm, K. Unterrainer, and E. Gornik, Phys. Rev. B **39**, 6212 (1989).